ACS Partner Journal

CHEMICAL & BIOMEDICAL IMAGING

pubs.acs.org/ChemBioImaging

Article

Engineering Isomeric AIEgens Containing Tetraphenylpyrazine for Dual Memory Storage

Zicheng Liu, Wenhao Wang, Hongfei Liao, Runfeng Lin, Xiang He, Canze Zheng, Changsheng Guo, Hongguang Liu,* Hai-Tao Feng, and Ming Chen*

Cite This: *Chem. Biomed. Imaging* 2024, 2, 117−125

Read Online

ACCESS | Metrics & More | Article Recommendations | Supporting Information

ABSTRACT: Tetraphenylpyrazine (TPP) is a promising heterocycle-based aggregation-induced emission luminogen (AIEgen) which has sparked multiple applications in organic light-emitting diodes, sensors, and biotherapy. However, the utility of it in developing information storage materials is relatively rare. Moreover, TPP is mostly employed as an electronic acceptor in molecular design, while the consideration of it as an electronic donor is attractive in studies which may provide a full understanding of its property to tailor the materials. In this work, we synthesize three TPP-based molecules by decorating it with acrylonitrile and isomeric pyridine units, which show AIE behavior by property inheritance from their parent unit. Interestingly, the effective intramolecular charge transfer takes place from the TPP electronic donor to the acrylonitrile and pyridine electronic acceptor, therefore inducing a remarkable solvatochromic effect as the solvent polarity improves. Moreover, it is revealed that the isomeric effect of the nitrogen atom in the pyridines may pose an influence on the absorption, solvatochromism, and AIE behavior. In addition, the acrylonitrile and pyridine groups are reactive to light and acid−base stimuli with irreversible and reversible responses, respectively. Combined with the high light-harvesting ability of these AIEgens, they show great potential in the stimuli-responsive materials for dual information storage.

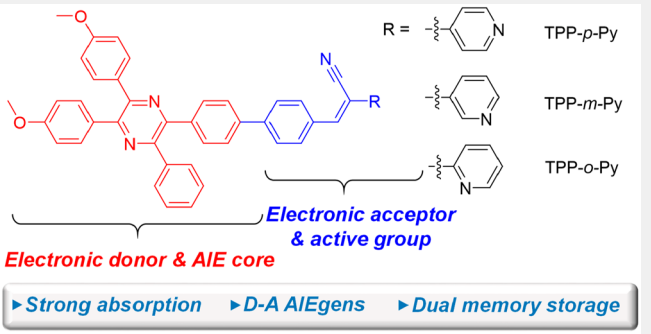

KEYWORDS: *aggregation-induced emission, tetraphenylpyrazine, intramolecular charge transfer, stimuli response, information storage materials*

INTRODUCTION

Stimuli-responsive materials for information storage have attracted considerable attention due to their potential applications in anticounterfeiting, memory chips, logical operation, and information security.[1−6] As the information is mainly obtained visually, the manipulation of absorption has been regarded as the most viable approach to input the information. However, it always encounters the drawbacks of low sensitivity and bad contrast.[7,8] Meanwhile, its poor regulation makes it hard to achieve versatile applications in complex occasions. By contrast, the fluorescent materials are naturally endowed with the merits of high brightness and excellent imaging ability.[9−11] Moreover, their emissions can be finely tuned by thoughtful structural design.[12−14] Thus, the utilization of fluorescent materials exhibits a significant advantage in the application of information storage, and actually has aroused extensive research interest over the past decades. Despite the different fluorescent materials such as organic dyes, organic-metal complexes, and quantum dots which can be employed, most of them suffer from the aggregation-caused quenching (ACQ) effect.[15−20] As aggregation is an intrinsic process of substance and most of the luminescent materials are used in the aggregate state, such an adverse effect has severely hampered their practical applications. Fortunately, aggregation-induced emission luminogens (AIEgens) could utilize aggregation to play a positive instead of negative role in enhancing luminescence, which can resolve such problems thoroughly.[21−24] This feature has dramatically promoted the development of functional fluorescent materials with applications in the fields of organic light-emitting diodes (OLEDs), bioimaging, therapy, and smart materials.[25−30]

Tetraphenylpyrazine (TPP) is a heterocycle luminogen with its AIE property first revealed in 2015.[31] Due to the excellent properties such as facile synthesis, good stability, unique nitrogen binding site, and tunable electronic property, many applications have been developed based on this building block.[32−35] For example, the decoration of phenanthroimida-

Received: April 11, 2023
Revised: May 12, 2023
Accepted: May 17, 2023
Published: June 6, 2023

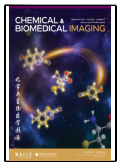

Scheme 1. Synthetic Route to TPP-Based AIE Isomers and the Roles of Each Unit in the Molecules

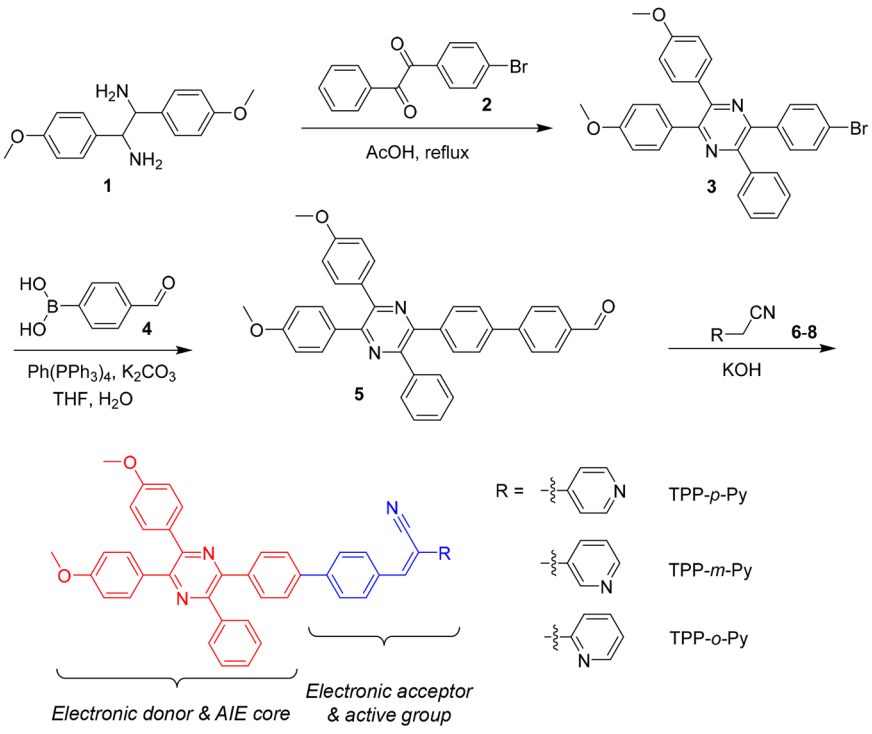

zole-based group onto TPP can give a sky blue donor−acceptor (D-A) type AIEgen with its fabricated OLED showing an external quantum efficiency as high as 4.85%.[36] Moreover, when the strong electronic donor of triphenylamine is attached to TPP, a remarkable D−A effect can be realized in AIEgens, showing an obvious solvatochromic effect.[37] Such push−pull electron effects can benefit an effective intramolecular charge transfer, whereas a two-photon excitation property can be obtained with the absorption cross section up to 480 GM at 800 nm. Yin et al. developed metal−organic frameworks (MOFs) with Ln^{3+} ions (e.g., Eu^{3+}, Tb^{3+}, and Gd^{3+}) and tetracarboxyl-substituted TPP as centers and ligand, respectively.[38] The dual emission behavior from the ligand, and metals can be tuned by changing the metal centers. More interestingly, the Eu^{3+}-MOF can act as a ratiometric fluorescent probe to detect arginine with a high sensitivity due to the specific hydrogen bond formation between the guanidine group of the amino acid and the nitrogen atom of TPP. Recently, we also prepared polymer photosensitizers (PSs) by a catalyst-free click reaction of tetraalkyne-substituted TPP with aryl thiols.[39] The PS can cause an excellent photodynamic therapy effect toward cancer cells under two-photon excitation, while the introduction of the TPP unit has a positive effect on both the photosensitization and two-photon behaviors. Despite the different applications discussed above, the utility of TPP in designing stimuli-responsive materials for information storage has been less investigated. Most of these examples are focused on molecular design with TPP as the electronic acceptor because of the strong electron affinity of the aromatic heterocycle.[40−44] It is still desirable to reversibly utilize it as an electronic donor in structural design, and carrying out such a study may provide deep insight into developing the functional material based on a full understanding of its property.

In this work, by modifying TPP with acrylonitrile and isomeric pyridine units, three AIEgens named TPP-*p*-Py, TPP-*m*-Py, and TPP-*o*-Py are obtained (Scheme 1). These AIEgens show strong absorptions at ∼370 nm with molar absorptivities in the range from 7.1×10^4 to 7.7×10^4 cm^{-1} L mol^{-1} in THF. Moreover, their THF solution gives strong yellow-green emissions which can be obviously red-shifted with the addition of water due to the twisted intramolecular transfer (TICT) effect. However, the aggregates can be formed in THF/water mixtures with a high water fraction (f_w) and show tunable aggregation-induced emissions, indicative of a property inheritance from the TPP unit. By comparison, a remarkable positive solvatochromic effect with an emission shift of more than 200 nm can be obtained in the *para*-position isomer with the change of the localized state to TICT emissions, which is derived from the effect of solvent polarity on the molecular excited states. Our study reveals that the isomeric effect brought by the nitrogen position in the pyridines can pose an effect on photophysical properties such as absorption, solvatochromism, and AIE effect, which provides a clue to precise tuning of the molecular properties. The theoretical calculation reveals that the charge transfer mainly comes from the TPP unit to the acrylonitrile and pyridine units. Thus, TPP is reversibly employed as an electronic donor in this study. Moreover, the modified groups of acrylonitrile and pyridine are active to light and acid−base stimuli with irreversible and reversible responses, respectively. This makes them easy to be fabricated as fluorescent strips for recording information with dual memory storage. Thus, the present work has established a study of TPP-based AIEgens affected by the electronic structure and the isomeric effect, and paved the way for their application as information storage materials.

https://doi.org/10.1021/cbmi.3c00048
Chem. Biomed. Imaging 2024, 2, 117−125

RESULTS AND DISCUSSION

The molecules are prepared on the basis of a bromo-substituted TPP derivative (**3**) which is synthesized by a cyclization reaction of 1,2-bis(4-methoxyphenyl)ethane-1,2-diamine (**1**) with 1-(4-bromophenyl)-2-phenylethane-1,2-dione (**2**) in acetic acid. A Suzuki coupling reaction of **3** with 4-formylphenylboronic acid (**4**) in the presence of $Pd(PPh_3)_4$ can readily afford an intermediate of **5**, followed by a Knoevenagel condensation reaction with benzonitriles (**6**–**8**) to generate three isomers, namely, TPP-*p*-Py, TPP-*m*-Py, and TPP-*o*-Py, respectively (Scheme 1). The products are obtained with a satisfactory yield with their structures well characterized by NMR and HRMS spectroscopies (Figures S1–S13). Thermogravimetric (TGA) analysis indicated that these molecules possess temperatures of 376, 274, and 373 °C, respectively, at 5% weight loss, suggestive of good thermal stability (Figure S14). These molecules can be generally regarded as a decoration of the TPP core with acrylonitrile and pyridine units. Meanwhile, the nitrogen atom shows isomeric substitutions in the pyridine groups which may provide information for tuning the photophysical properties influenced by such an effect.

The absorption of these isomers is investigated via UV–vis spectra (Figure 1). The result indicates that they possess a

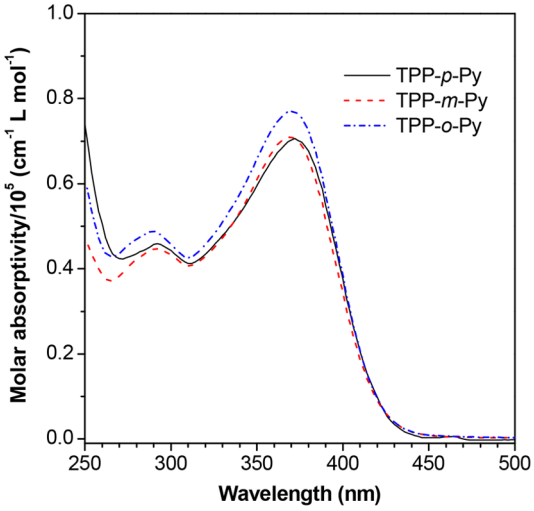

Figure 1. UV–vis spectra of AIE isomers in THF, [dye] = 10 μM.

similar absorption profile in THF with two peaks located at ~370 and ~291 nm, which are attributable to the charge-transfer and local state excitations in the molecules, respectively. However, there are some differences between them. The absorption maximum of TPP-*p*-Py is a bit redder than that of TPP-*m*-Py and TPP-*o*-Py. It suggests that the existence of nitrogen in the *para*-position is in favor of charge transfer determined by the stronger inductive effect. Moreover, the absorption intensity of TPP-*o*-Py is somewhat higher than that of the others, proving that in the molecule the electronic effect is less affected by the *ortho*-position substitution and fewer charge-transfer effects are involved to decrease the electron transition. It is noteworthy that the molar absorptivities of these molecules are in the range from 7.1×10^4 to 7.7×10^4 cm^{-1} L mol^{-1}, which is much higher than that of its TPP unit (2.4×10^4 cm^{-1} L mol^{-1}).[31] It is because the incorporated acrylonitrile unit shows a good planarity which may make a contribution to the overall molecular conjugation for effective excitation. The high light-harvesting ability of AIEgens is particularly useful in practical applications.[45]

Since TPP is a typical AIEgen, what about the luminescent property of TPP-*p*-Py, TPP-*m*-Py, and TPP-*o*-Py affected by the substituents? To answer this question, their photoluminescence (PL) spectra in THF/water mixtures with different water fractions (f_w) are studied (Figure 2A–C). Different from TPP, these luminogens emit obviously in THF with peaks at 561, 527, and 519 nm, respectively, which have a remarkable red-shift in comparison to TPP (~400 nm).[31] It suggests that a notable D–A effect has been generated based on the structural derivation. Moreover, a much redder emission can be found in TPP-*p*-Py by comparison to TPP-*m*-Py and TPP-*o*-Py because the D–A effect has been strengthened by the *para*-position substitution of the nitrogen atom in the pyridine.

After the addition of water, all the molecules show gradually bathochromic-shifted but quenched emissions as f_w increases from 0 to 60%. The red-shift of their emission wavelengths are recorded as ~44, 53, and 52 nm, respectively (Figure 2A–C). This is because the polarity of the mixed solvent is improved with the addition of water. The higher polarity will give rise to a stronger intramolecular charge transfer between the D–A pair brought on by a twisted molecular conformation, whereas the TICT effect may induce broader spectra with redder but weaker emissions.[46−48] Moreover, TPP-*p*-Py exhibits a very obvious quenching in the emissions as polarity improves because a stronger TICT effect can produce in the molecules with a more evident D–A effect. With high f_w from 70% to 95%, molecular aggregation occurs which is proved by the observed particle sizes of ~400–1400 nm from the dynamic light scattering analysis (Figure S15). The emission properties affected by the solvating effect are thus weakened. Instead, the aggregation-induced emissions with a hypochromatic-shift effect can be evoked by the suppression of intramolecular motions in the aggregates (Figure 2). However, they show a different AIE behavior probably due to the disparate aggregate-state structure caused by the isomeric effect. The absolute quantum yields (Φ_F) of these AIEgens in the film state are recorded as 16.8%, 9.24%, and 9.64%, respectively, by an integrating sphere. The higher Φ_F values also correspond to the longer lifetimes of 4.56, 2.98, and 2.74 ns collected via the transient PL spectra. Thus, the luminescent behavior of these AIEgens in both the solution and aggregate states can be profoundly affected by the structural factor.

To have a better understanding of their electronic property, the solvatochromic effect is investigated in different solvents with a wide polarity range (Figure 3). The UV–vis spectra reveal that, regardless of various solvents, they all also show similar absorption profiles and maximum wavelengths, indicating that their ground-state properties have been less influenced (Figures 3A and S16). In sharp contrast, a remarkable change of emissions can be observed in the PL spectra (Figures 3B and S17). For example, TPP-*p*-Py displays a blue emission at 471 nm in a nonpolar solvent of hexane, while the emission almost becomes redder as the solvent polarity parameter (Δf) increases. In the high polar solvent of acetonitrile, a very weak emission is recorded at 674 nm, which is more than 200 nm redder than that in hexane, suggestive of a notable solvatochromic behavior caused by the D–A effect. For TPP-*m*-Py and TPP-*o*-Py, they show an emission behavior close to that of TPP-*p*-Py in the non- or low polar solvents but

https://doi.org/10.1021/cbmi.3c00048
Chem. Biomed. Imaging 2024, 2, 117–125

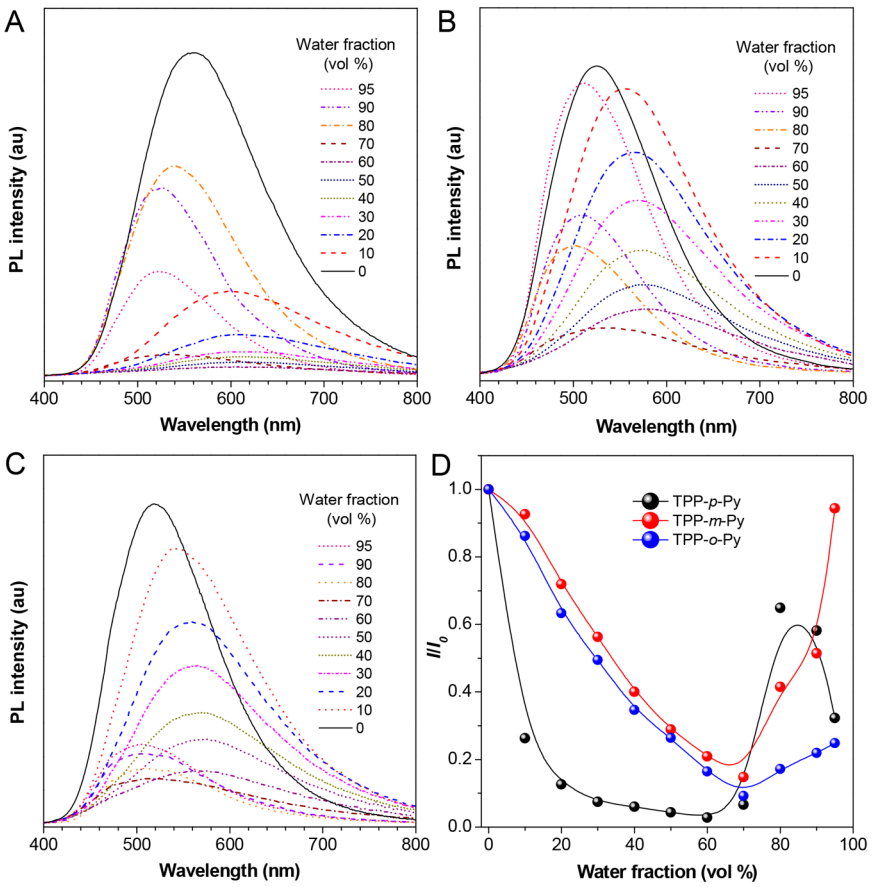

Figure 2. PL spectra of (A) TPP-*p*-Py, (B) TPP-*m*-Py, and (C) TPP-*o*-Py in THF/water mixture with different f_w, [dye] = 10 μM, λ_{ex} = 370 nm; (D) Changes of relative PL intensities (I/I_0) versus f_w in these AIEgens.

a much different behavior in the high polar solvents. The changes of their emission wavelengths are recorded as ∼143 and 150 nm, respectively, which are much smaller than that of TPP-*p*-Py due to a weaker D−A effect. Moreover, all molecules show narrower emissions in the non- or low polar solvents because the localized-state emissions dominate as their D−A conformations are more planar and stabilized by the solvents. However, in the higher polarity solvents, the TICT emissions are predominant as reflected by their long wavelength and wide emissions. Thus, their excited-state properties can be greatly affected by the solvent polarity. We also evaluate the influence of Δf on the Stokes shift using the Lippert−Mataga equation:[49]

$$\Delta\nu \equiv \nu_{ab} - \nu_{em} = \frac{2\Delta f}{hca^3}(\mu_e - \mu_g)^2 + \text{const}$$

$$\Delta f = \frac{\varepsilon - 1}{2\varepsilon + 1} - \frac{n^2 - 1}{2n^2 + 1}$$

where $\Delta\upsilon$ is the Stokes shift, h is the Planck constant, c is the speed of light, a is the radius of the luminogens, μ_e and μ_g are the dipole moments in the excited and ground states, and ε and n are the dielectric constant and refractive index of the solvent, respectively. From the plots of $\Delta\upsilon$ versus Δf, it is clear that these molecules possess an obvious positive slope after linear fitting, with the values deduced to be as large as 19 015, 16 029 and 16 002, respectively (Figure 3C). The solvating effect of TPP-*p*-Py is much larger than those of TPP-*m*-Py and TPP-*o*-Py, which are almost the same (Figure 3D). This is in accordance with the above discussion that the *para*-position isomerization may pose the strongest D−A effect to produce a better positive solvating effect than the other substituents.

The theoretical calculation at the B3LYP/6-31G(d,p) level reveals that these molecules possess a very similar electronic structure (Figure 4). It is clear that their highest occupied molecular orbitals (HOMOs) are centered at the TPP unit as well as the oxygen atom from the attached methoxy groups, whereas the lowest unoccupied molecular orbitals (LUMOs) are mainly distributed on the pyridines, acrylonitrile units, and linked phenyl rings. It suggests an obvious intramolecular charge transfer from the TPP-based electronic donors to the pyridine and acrylonitrile electronic acceptors. It is worth noting that TPP is normally used as an acceptor unit in the molecular design. The present work exhibits a reversible utility of TPP as electronic donor as its electron affinity is much weaker than that of pyridines and acrylonitrile units. Moreover, the similar electronic structure may lead to a close energy gap (ΔE). However, the ΔE of TPP-*p*-Py is a bit smaller than that of TPP-*m*-Py and TPP-*o*-Py which are relatively approximate. This verifies that the D−A effect of TPP-*p*-Py is enhanced by the *para*-position substitution, which in turn induces a more apparent charge-transfer effect.

Besides the electron-withdrawing property bestowed by the modified groups, they also show obvious reactivity which may aid to develop the related functionalities. Our study reveal that these AIEgens are sensitive to light irradiation. Taking TPP-*p*-Py as an example, its aggregates formed in THF/water with f_w = 90% show a strong emission at 522 nm. Upon irradiation

https://doi.org/10.1021/cbmi.3c00048
Chem. Biomed. Imaging 2024, 2, 117−125

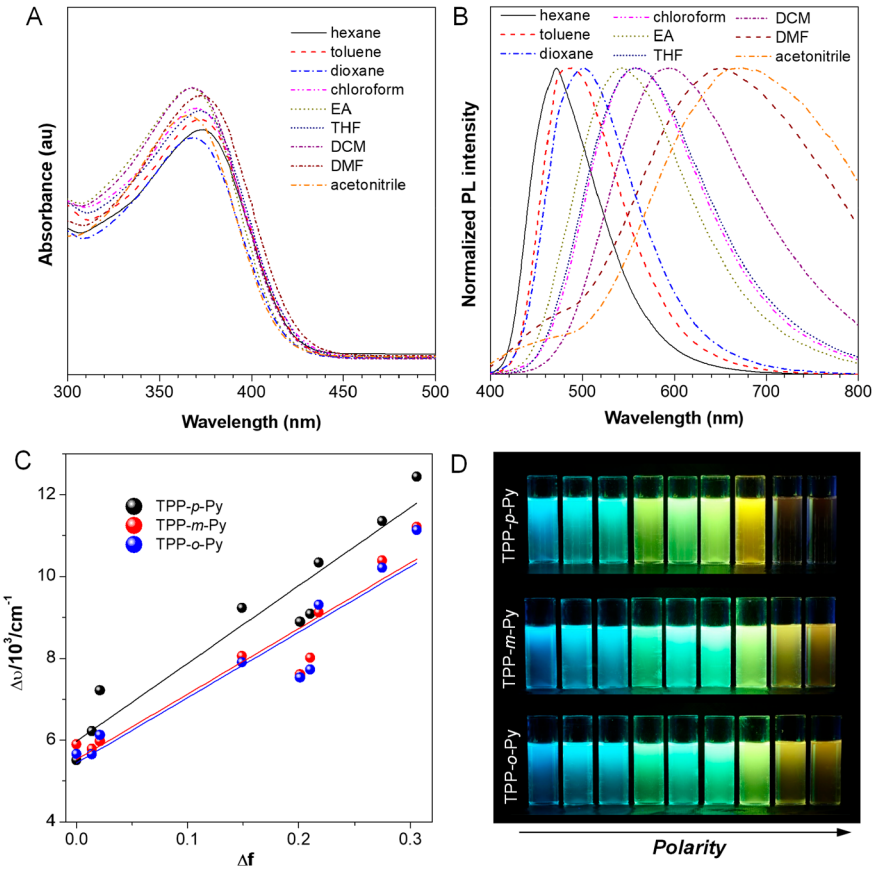

Figure 3. (A) UV−vis and (B) PL spectra of TPP-*p*-Py in different solvents, [dye] = 10 μM, λ_{ex} = 370 nm. (C) Plot of Stokes shift ($\Delta\upsilon$) of AIE isomers versus Δf of solvents. (D) Photographs of AIE isomers in different solvents taken under 365 nm UV light.

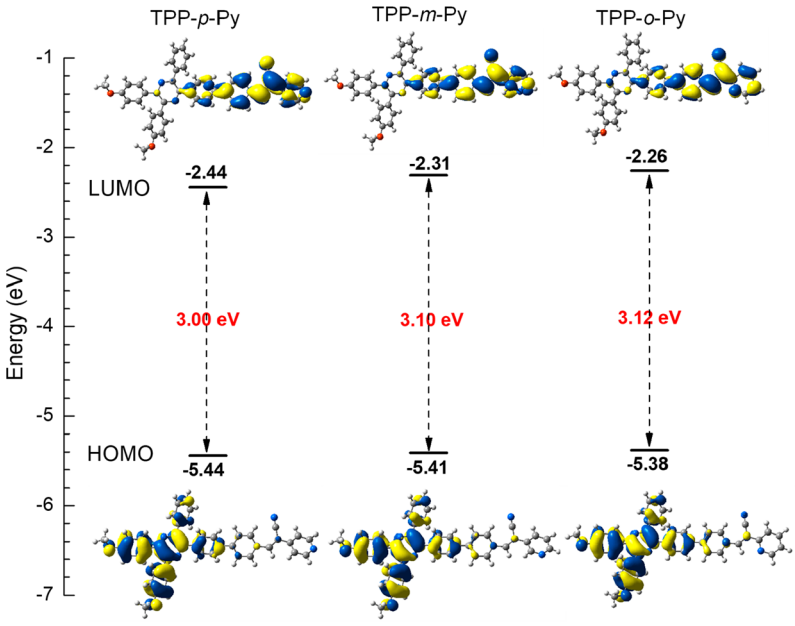

Figure 4. Molecular orbitals, energy levels, and energy gaps based on S_0 conformation of AIE isomers optimized at B3LYP/6-31G (d, p) level.

with 365 nm UV light, the emission drops sharply within 1 h accompanied by a gradual blue-shift effect. Afterward, the decrease becomes slow and nearly reaches a constant after 2 h (Figure 5A). A similar photoresponsive behavior has also been observed in TPP-*m*-Py and TPP-*o*-Py despite their different attenuation rates and reaction extent affected by the isomeric effect (Figure 5B−D). Normally, there are possibly two approaches to explain the photoresponsive behavior. One is the isomerization of the double bond in the acrylonitrile unit caused by the light excitation, while the other is the

https://doi.org/10.1021/cbmi.3c00048
Chem. Biomed. Imaging 2024, 2, 117−125

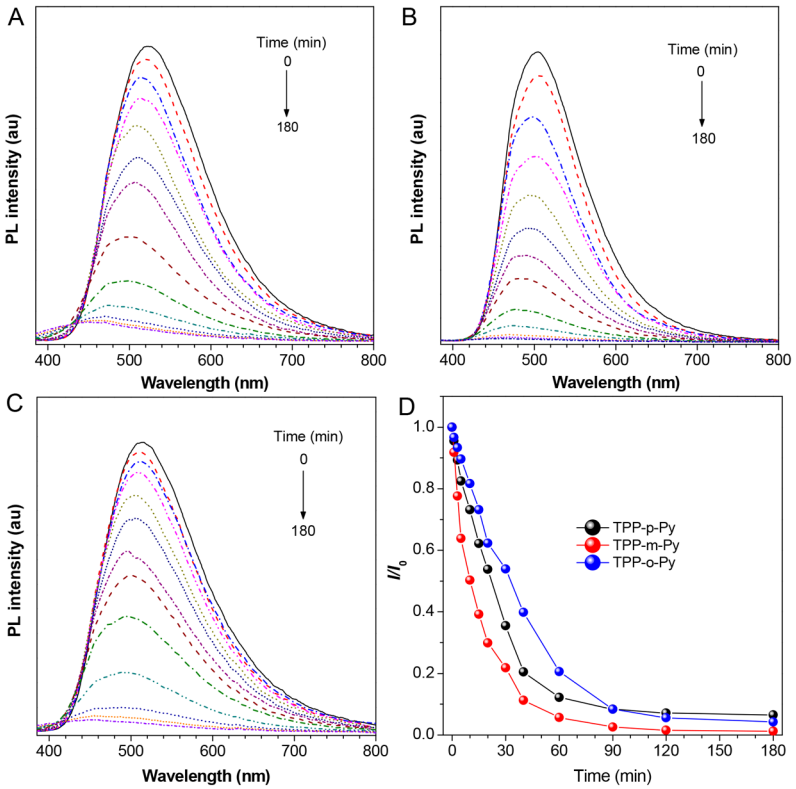

Figure 5. PL spectra of (A) TPP-*p*-Py, (B) TPP-*m*-Py, and (C) TPP-*o*-Py in THF/water mixtures with f_w = 90% under continuous UV light irradiation, [dye] = 10 μM, λ_{ex} = 370 nm. (D) Changes relative PL intensities (I/I_0) versus time in AIEgens.

photodimerization of double bonds between the adjacent molecules.[50,51] For the photoisomerization reaction, a less allochroic phenomenon should be generated as the *Z*/*E* isomerization may not lead to an obvious influence on the conjugation effect. However, the PL spectra of AIEgens under prolonged exposure to UV light suggest a much more hypochromatic-shifted emission at ∼450 nm, which is close to that from the TPP-based unit (Figure 5A−C).[31] The UV−vis spectra of the aggregates show that their maximum absorption at ∼365 nm has decreased obviously with time under light irradiation (Figure S18). On the other hand, such photostimuli responses are found to be more obvious in the aggregate state than in the solution state, which may provide a favorable condition for the intermolecular reactions. All these suggest that the photodimerization reaction may dominate to break the double bond and remove the D−A effect which can affect the emission properties. The emission quenching is mainly due to the free volume produced by the photodimerization reaction to break the molecular array which can remarkably enhance the nonradiative transition after excitation.[52]

Moreover, the pyridine groups existing in the AIEgens may endow them with remarkable acid−base response properties (Figure 6). For example, the pristine powders of TPP-*p*-Py, TPP-*m*-Py, and TPP-*o*-Py emit at 512, 506, and 536 nm, respectively. After being fumed with hydrochloric acid (HCl) vapor, the obvious red-shift of emissions by 88, 61, and 47 nm can be recorded in these powders.

However, such changes can be recovered to an obvious extent by retreating the powders with the trimethylamine (TEA) vapor (Figure 6A−C). Moreover, the experiments during the 5 cycles of acid−base treatments indicate a good fatigue resistance to such a stimuli response (Figure 6D). As pyridine is a basic group, it is easily protonated by HCl to form the pyridine salt group which shows a much stronger electron affinity to affect the electronic property. However, such a process is normally recoverable by a deprotonation reaction with TEA. The effect of protonation on the electronic property is verified by theoretical investigations where the LUMO energy levels were reduced by 0.42, 0.34, and 0.35 eV in TPP-*p*-Py, TPP-*m*-Py, and TPP-*o*-Py, respectively, after interacting with HCl, while those of HOMO energy levels change less (Figure S19). Thus, ΔE can be obviously decreased to red-shift the emissions. In comparison, the variation in TPP-*p*-Py is much larger than the others due to the *para*-position effect which can induce a more effective intramolecular charge transfer. Thus, the isomeric effect of these AIEgens makes the acid−base response behavior controllable, which is extremely useful in the development of smart functional materials.

Because both the reversible and irreversible stimuli-responsive behaviors have been realized in these AIEgens, they are very promising for applications as information storage materials. Herein, the memory strips are fabricated by immersing the silica gel plate into the solution of AIEgens, followed by volatilizing the solvent in the fume hood. The good adsorptivity of the silica gel makes the fluorogens fully loaded and well dispersed, which is beneficial to improve the sensitivity for the fluorescent response. The results exhibit that these strips give a greenish emission with high uniformity under 365 nm UV light irradiation (Figure 7). While exposing them to the HCl vapor through a mask, a very clear word of "JNU" can be recorded which shows much redder but weaker emissions due to the protonation effect. However, this information can be almost erased by retreating the strips

https://doi.org/10.1021/cbmi.3c00048
Chem. Biomed. Imaging 2024, 2, 117−125

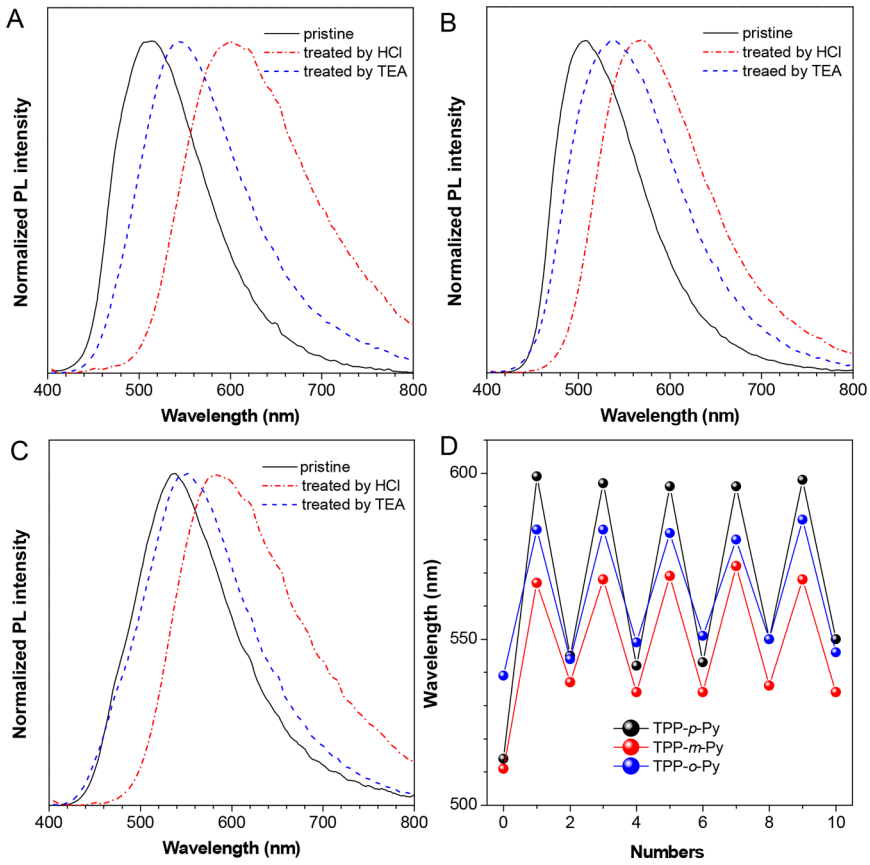

Figure 6. PL spectra of powders of (A) TPP-*p*-Py, (B) TPP-*m*-Py, and (C) TPP-*o*-Py with different treatments, λ_{ex} = 370 nm. (D) Changes of emission wavelengths of AIE isomers during 5 cycles of acid–base responses.

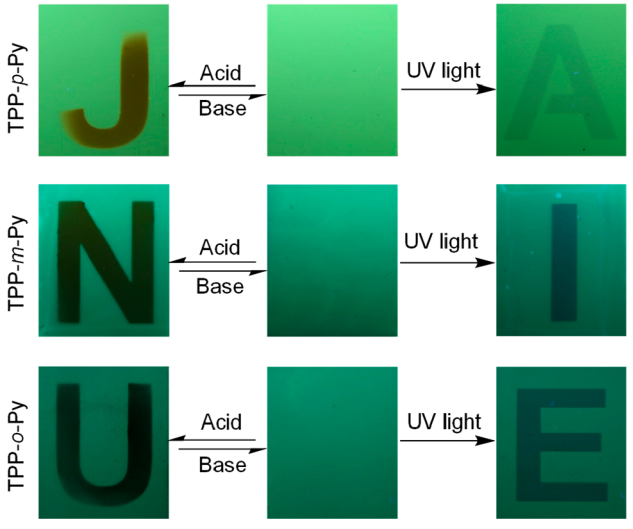

Figure 7. Dual information storage with AIE isomers under acid–base and UV light responses.

with the TEA vapor. This suggests that the strips are suitable for reversible memory storage in burning information. Moreover, such strips can be also utilized for recording the information with a permanent memory. For example, by continuous irradiation of them with UV light through another mask, the distinct pattern of "AIE" with weak emissions can be generated by virtue of the photodimerization reaction, while such a record cannot be removed afterward. Thus, with these AIEgens, the reversible and irreversible memory storage can be achieved to meet the different applications for information storage.

CONCLUSIONS

In this work, based on a building block of TPP, we obtain three AIE isomers by decorating them with acrylonitrile and pyridine units, while their photophysical properties are affected by the substitution position of the nitrogen atom in the pyridines. These AIEgens show strong absorptions with molar absorptivities in the range of 7.1×10^4–7.7×10^4 cm^{-1} L mol^{-1} in THF due to the artful molecular design. Moreover, the structural decoration has obviously red-shifted their emissions, and a remarkable solvatochromic phenomenon caused by the TICT effect is found in solvent with increasing polarity, while such behavior is suppressed by aggregation to induce an enhanced emission. The molecule with *para*-position substitution has a more obvious intramolecular charge transfer effect than the other substituents to affect the molecular absorption, solvatochromism, and AIE effect. Theoretical calculation reveals that an evident intramolecular charge transfer has taken place from the TPP unit to the acrylonitrile and pyridine units, suggestive of the utility of TPP as an electronic donor for molecular design, which is different from most previous reports. Besides the electron-withdrawing property of the acrylonitrile and pyridine units, they can act as active groups to separately undergo photoinduced dimerization and protonation reactions, while the irreversible and reversible fluorescence responses by light and acid–base

https://doi.org/10.1021/cbmi.3c00048
Chem. Biomed. Imaging 2024, 2, 117–125

stimuli can be easily achieved. These features allow the AIEgens to be fabricated as fluorescent strips to record information with dual memory storage. This work not only provides a deep understanding of TPP-based AIEgens affected by electronic structure as well as isomeric effects, but also broadens their applications as information storage materials.

■ ASSOCIATED CONTENT

Supporting Information

The Supporting Information is available free of charge at https://pubs.acs.org/doi/10.1021/cbmi.3c00048.

^{1}H NMR, ^{13}C NMR, and HRMS spectroscopies, TGA curves, PL spectra, UV−vis spectra, and theoretical results (PDF)

■ AUTHOR INFORMATION

Corresponding Authors

Hongguang Liu − *College of Chemistry and Materials Science, Jinan University, Guangzhou 510632, China;* orcid.org/0000-0003-0736-8054; Email: hongguang_liu@jnu.edu.cn

Ming Chen − *College of Chemistry and Materials Science, Jinan University, Guangzhou 510632, China; Guangdong Provincial Key Laboratory of Luminescence from Molecular Aggregates, South China University of Technology, Guangzhou 510640, China;* orcid.org/0000-0003-4071-6604; Email: chenming@jnu.edu.cn

Authors

Zicheng Liu − *College of Chemistry and Materials Science, Jinan University, Guangzhou 510632, China*

Wenhao Wang − *College of Chemistry and Materials Science, Jinan University, Guangzhou 510632, China*

Hongfei Liao − *College of Chemistry and Materials Science, Jinan University, Guangzhou 510632, China*

Runfeng Lin − *College of Chemistry and Materials Science, Jinan University, Guangzhou 510632, China*

Xiang He − *College of Chemistry and Materials Science, Jinan University, Guangzhou 510632, China*

Canze Zheng − *College of Chemistry and Materials Science, Jinan University, Guangzhou 510632, China*

Changsheng Guo − *AIE Research Center, Shaanxi Key Laboratory of Photochemistry, College of Chemistry and Chemical Engineering, Baoji University of Arts and Sciences, Baoji 721013, China*

Hai-Tao Feng − *AIE Research Center, Shaanxi Key Laboratory of Photochemistry, College of Chemistry and Chemical Engineering, Baoji University of Arts and Sciences, Baoji 721013, China*

Complete contact information is available at: https://pubs.acs.org/10.1021/cbmi.3c00048

Notes

The authors declare no competing financial interest.

■ ACKNOWLEDGMENTS

This work was partially support by the National Natural Science Foundation of China (22275072), Guangdong Provincial Key laboratory of Luminescence from Molecular Aggregates (2019B030301003), and Scientific and Technological Innovation Team of Shaanxi Province (2022TD-36).

■ REFERENCES

(1) Theato, P.; Sumerlin, B. S.; O'Reilly, R. K.; Epps, T. H., III Stimuli responsive materials. *Chem. Soc. Rev.* **2013**, *42*, 7055−7056.

(2) Lou, K.; Hu, Z.; Zhang, H.; Li, Q.; Ji, X. Information Storage Based on Stimuli-Responsive Fluorescent 3D Code Materials. *Adv. Funct. Mater.* **2022**, *32*, 2113274.

(3) Le, X.-X.; Lu, W.; He, J.; Serpe, M. J.; Zhang, J.-W.; Chen, T. Ionoprinting controlled information storage of fluorescent hydrogel for hierarchical and multi-dimensional decryption. *Sci. China Mater.* **2019**, *62*, 831−839.

(4) Wang, H.; Ji, X.; Page, Z. A.; Sessler, J. L. Fluorescent materials-based information storage. *Mater. Chem. Front.* **2020**, *4*, 1024−1039.

(5) Kahn, J. S.; Hu, Y.; Willner, I. Stimuli-Responsive DNA-Based Hydrogels: From Basic Principles to Applications. *Acc. Chem. Res.* **2017**, *50*, 680−690.

(6) Ng, K. K.; Shakiba, M.; Huynh, E.; Weersink, R. A.; Roxin, Á.; Wilson, B. C.; Zheng, G. Stimuli-Responsive Photoacoustic Nanoswitch for in Vivo Sensing Applications. *ACS Nano* **2014**, *8*, 8363−8373.

(7) Zuber, A.; Purdey, M.; Schartner, E.; Forbes, C.; van der Hoek, B.; Giles, D.; Abell, A.; Monro, T.; Ebendorff-Heidepriem, H. Detection of gold nanoparticles with different sizes using absorption and fluorescence based method. *Sensor Actuat B-Chem.* **2016**, *227*, 117−127.

(8) Goswami, S.; Sen, D.; Das, N. K. A New Highly Selective, Ratiometric and Colorimetric Fluorescence Sensor for Cu2+ with a Remarkable Red Shift in Absorption and Emission Spectra Based on Internal Charge Transfer. *Org. Lett.* **2010**, *12*, 856−859.

(9) Zhu, C.; Liu, L.; Yang, Q.; Lv, F.; Wang, S. Water-Soluble Conjugated Polymers for Imaging, Diagnosis, and Therapy. *Chem. Rev.* **2012**, *112*, 4687−4735.

(10) Wu, X.; Wang, R.; Kwon, N.; Ma, H.; Yoon, J. Activatable fluorescent probes for in situ imaging of enzymes. *Chem. Soc. Rev.* **2022**, *51*, 450−463.

(11) Hong, Y.; Geng, W.; Zhang, T.; Gong, G.; Li, C.; Zheng, C.; Liu, F.; Qian, J.; Chen, M.; Tang, B. Z. Facile Access to Far-Red Fluorescent Probes with Through-Space Charge-Transfer Effects for In Vivo Two-Photon Microscopy of the Mouse Cerebrovascular System. *Angew. Chem., Int. Ed.* **2022**, *61*, No. e202209590.

(12) Jiang, G.; Yu, J.; Wang, J.; Tang, B. Z. Ion-π interactions for constructing organic luminescent materials. *Aggregate* **2022**, *3*, e285.

(13) Zhu, H.; Fan, J.; Du, J.; Peng, X. Fluorescent Probes for Sensing and Imaging within Specific Cellular Organelles. *Acc. Chem. Res.* **2016**, *49*, 2115−2126.

(14) Kim, J. S.; Quang, D. T. Calixarene-Derived Fluorescent Probes. *Chem. Rev.* **2007**, *107*, 3780−3799.

(15) Green, A. P.; Buckley, A. Solid state concentration quenching of organic fluorophores in PMMA. *Phys. Chem. Chem. Phys.* **2015**, *17*, 1435−1440.

(16) Kim, S.; Pudavar, H. E.; Bonoiu, A.; Prasad, P. N. Aggregation-Enhanced Fluorescence in Organically Modified Silica Nanoparticles: A Novel Approach toward High-Signal-Output Nanoprobes for Two-Photon Fluorescence Bioimaging. *Adv. Mater.* **2007**, *19*, 3791−3795.

(17) Petrova, O. B.; Avetisov, R. I.; Avetisov, I. K.; Mushkalo, O. A.; Khomyakov, A. V.; Cherednichenko, A. G. Hybrid materials based on organic luminophores in inorganic glass matrix. *Opt. Spectrosc.* **2013**, *114*, 886−889.

(18) Zhao, B.; Zhang, H.; Miao, Y.; Wang, Z.; Gao, L.; Wang, H.; Hao, Y.; Xu, B.; Li, W. Low turn-on voltage and low roll-off rare earth europium complex-based organic light-emitting diodes with exciplex as the host. *J. Mater. Chem. C* **2017**, *5*, 12182−12188.

(19) Noh, M.; Kim, T.; Lee, H.; Kim, C.-K.; Joo, S.-W.; Lee, K. Fluorescence quenching caused by aggregation of water-soluble CdSe quantum dots. *Colloids Surf. A Physicochem. Eng. Asp.* **2010**, *359*, 39−44.

(20) Wei, W.; Chen, G.; Baev, A.; He, G. S.; Shao, W.; Damasco, J.; Prasad, P. N. Alleviating Luminescence Concentration Quenching in Upconversion Nanoparticles through Organic Dye Sensitization. *J. Am. Chem. Soc.* **2016**, *138*, 15130−15133.

(21) Luo, J.; Xie, Z.; Lam, J. W. Y.; Cheng, L.; Chen, H.; Qiu, C.; Kwok, H. S.; Zhan, X.; Liu, Y.; Zhu, D.; Tang, B. Z. Aggregation-induced emission of 1-methyl-1,2,3,4,5-pentaphenylsilole. *Chem. Commun.* **2001**, 1740−1741.
(22) Hu, F.; Liu, B. Organelle-specific bioprobes based on fluorogens with aggregation-induced emission (AIE) characteristics. *Org. Biomol. Chem.* **2016**, *14*, 9931−9944.
(23) Xu, M.; Wang, X.; Wang, Q.; Hu, Q.; Huang, K.; Lou, X.; Xia, F. Analyte-responsive fluorescent probes with AIE characteristic based on the change of covalent bond. *Sci. China Mater.* **2019**, *62*, 1236−1250.
(24) Chen, C.; Ni, X.; Jia, S.; Liang, Y.; Wu, X.; Kong, D.; Ding, D. Massively Evoking Immunogenic Cell Death by Focused Mitochondrial Oxidative Stress using an AIE Luminogen with a Twisted Molecular Structure. *Adv. Mater.* **2019**, *31*, 1904914.
(25) Wei, Q.; Fei, N.; Islam, A.; Lei, T.; Hong, L.; Peng, R.; Fan, X.; Chen, L.; Gao, P.; Ge, Z. Small-Molecule Emitters with High Quantum Efficiency: Mechanisms, Structures, and Applications in OLED Devices. *Adv. Optical Mater.* **2018**, *6*, 1800512.
(26) Yang, J.; Huang, J.; Li, Q.; Li, Z. Blue AIEgens: approaches to control the intramolecular conjugation and the optimized performance of OLED devices. *J. Mater. Chem. C* **2016**, *4*, 2663−2684.
(27) Chen, M.; Kwok, R. T. K.; Tang, Y.; Ding, D. Strategies in boosting photosensitization for biomedical applications. *Sci. China Chem.* **2022**, *65*, 647−649.
(28) Li, C.; Jiang, G.; Yu, J.; Ji, W.; Liu, L.; Zhang, P.; Du, J.; Zhan, C.; Wang, J.; Tang, B. Z. Fluorination Enhances NIR-II Emission and Photothermal Conversion Efficiency of Phototheranostic Agents for Imaging-Guided Cancer Therapy. *Adv. Mater.* **2023**, *35*, 2208229.
(29) Yao, W.; Tebyetekerwa, M.; Bian, X.; Li, W.; Yang, S.; Zhu, M.; Hu, R.; Wang, Z.; Qin, A.; Tang, B. Z. Materials interaction in aggregation-induced emission (AIE)-based fluorescent resin for smart coatings. *J. Mater. Chem. C* **2018**, *6*, 12849−12857.
(30) Feng, L.; Li, C.; Liu, L.; Chen, X.; Jiang, G.; Wang, J.; Tang, B. Z. A Facile Structural Isomerization-Induced 3D Spatial D-A Interlocked Network for Achieving NIR-II Phototheranostic Agents. *Angew. Chem., Int. Ed.* **2022**, *61*, No. e202212673.
(31) Chen, M.; Li, Z.; Nie, H.; Tong, J.; Yan, L.; Xu, B.; Sun, J. Z.; Tian, W.; Zhao, Z.; Qin, A.; Tang, B. Z. Tetraphenylpyrazine-based AIEgens: facile preparation and tunable light emission. *Chem. Sci.* **2015**, *6*, 1932−1937.
(32) Chen, M.; Chen, R.; Shi, Y.; Wang, J.; Cheng, Y.; Li, Y.; Gao, X.; Yan, Y.; Sun, J. Z.; Qin, A.; Kwok, R. T. K.; Lam, J. W. Y.; Tang, B. Z. Malonitrile-Functionalized Tetraphenylpyrazine: Aggregation-Induced Emission, Ratiometric Detection of Hydrogen Sulfide, and Mechanochromism. *Adv. Funct. Mater.* **2018**, *28*, 1704689.
(33) Chen, M.; Liu, J.; Liu, F.; Nie, H.; Zeng, J.; Lin, G.; Qin, A.; Tu, M.; He, Z.; Sung, H. H. Y.; Williams, I. D.; Lam, J. W. Y.; Tang, B. Z. Tailoring the Molecular Properties with Isomerism Effect of AIEgens. *Adv. Funct. Mater.* **2019**, *29*, 1903834.
(34) Gong, G.; Wu, H.; Zhang, T.; Wang, Z.; Li, X.; Xie, Y. Aggregation-enhanced emission in tetraphenylpyrazine-based luminogens: theoretical modulation and experimental validation. *Mater. Chem. Front.* **2021**, *5*, 5012−5023.
(35) Gong, G.; Dong, X.; Ran, X.; Mu, J.; Zhang, T.; Wang, Z. Theoretical insights into the central "acceptor" bridge function on the whole visible light and near-infrared emission in tetraphenylpyrazine-based luminogens. *New J. Chem.* **2022**, *46*, 16932−16940.
(36) Wu, H.; Pan, Y.; Zeng, J.; Du, L.; Luo, W.; Zhang, H.; Xue, K.; Chen, P.; Phillips, D. L.; Wang, Z.; Qin, A.; Tang, B. Z. Novel Strategy for Constructing High Efficiency OLED Emitters with Excited State Quinone-Conformation Induced Planarization Process. *Adv. Optical Mater.* **2019**, *7*, 1900283.
(37) Chen, M.; Nie, H.; Song, B.; Li, L.; Sun, J. Z.; Qin, A.; Tang, B. Z. Triphenylamine-functionalized tetraphenylpyrazine: facile preparation and multifaceted functionalities. *J. Mater. Chem. C* **2016**, *4*, 2901−2908.
(38) Yin, H.-Q.; Wang, X.-Y.; Yin, X.-B. Rotation Restricted Emission and Antenna Effect in Single Metal−Organic Frameworks. *J. Am. Chem. Soc.* **2019**, *141*, 15166−15173.
(39) Li, C.; Liu, J.; Hong, Y.; Lin, R.; Liu, Z.; Chen, M.; Lam, J. W. Y.; Ning, G.-H.; Zheng, X.; Qin, A.; Tang, B. Z. Click Synthesis Enabled Sulfur Atom Strategy for Polymerization-Enhanced and Two-Photon Photosensitization. *Angew. Chem., Int. Ed.* **2022**, *61*, No. e202202005.
(40) Feng, H.-T.; Zheng, X.; Gu, X.; Chen, M.; Lam, J. W. Y.; Huang, X.; Tang, B. Z. White-Light Emission of a Binary Light-Harvesting Platform Based on an Amphiphilic Organic Cage. *Chem. Mater.* **2018**, *30*, 1285−1290.
(41) Li, Y.; He, W.; Peng, Q.; Hou, L.; He, J.; Li, K. Aggregation-induced emission luminogen based molecularly imprinted ratiometric fluorescence sensor for the detection of Rhodamine 6G in food samples. *Food Chem.* **2019**, *287*, 55−60.
(42) Ying, X.-D.; Chen, J.-X.; Tu, D. Y.; Zhuang, Y. C.; Wu, D.; Shen, L. Tetraphenylpyrazine-Based Luminescent Metal−Organic Framework for Chemical Sensing of Carcinoids Biomarkers. *ACS Appl. Mater. Interfaces* **2021**, *13*, 6421−6429.
(43) Lin, H.; Chen, S.; Hu, H.; Zhang, L.; Ma, T.; Lai, J. Y. L.; Li, Z.; Qin, A.; Huang, X.; Tang, B. Z.; Yan, H. Reduced Intramolecular Twisting Improves the Performance of 3D Molecular Acceptors in Non-Fullerene Organic Solar Cells. *Adv. Mater.* **2016**, *28*, 8546−8551.
(44) Zou, Y.; Huang, K.; Zhang, X.; Qin, D.; Zhao, B. Tetraphenylpyrazine-Based Manganese Metal−Organic Framework as a Multifunctional Sensor for Cu^{2+}, Cr^{3+}, MnO^{4-}, and 2,4,6-Trinitrophenol and the Construction of a Molecular Logical Gate. *Inorg. Chem.* **2021**, *60*, 11222−11230.
(45) Hedley, G. J.; Ruseckas, A.; Samuel, I. D. W. Light Harvesting for Organic Photovoltaics. *Chem. Rev.* **2017**, *117*, 796−837.
(46) Grabowski, Z. R.; Rotkiewicz, K.; Rettig, W. Structural Changes Accompanying Intramolecular Electron Transfer: Focus on Twisted Intramolecular Charge-Transfer States and Structures. *Chem. Rev.* **2003**, *103*, 3899−4032.
(47) Sasaki, S.; Drummen, G. P. C.; Konishi, G.-i. Recent advances in twisted intramolecular charge transfer (TICT) fluorescence and related phenomena in materials chemistry. *J. Mater. Chem. C* **2016**, *4*, 2731−2743.
(48) Wu, C.-J.; Li, X.-Y.; Zhu, T.; Zhao, M.; Song, Z.; Li, S.; Shao, G.-G.; Niu, G. Exploiting the Twisted Intramolecular Charge Transfer Effect to Construct a Wash-Free Solvatochromic Fluorescent Lipid Droplet Probe for Fatty Liver Disease Diagnosis. *Anal. Chem.* **2022**, *94*, 3881−3887.
(49) Bagchi, B.; Oxtoby, D. W.; Fleming, G. R. Theory of the time development of the stokes shift in polar media. *Chem. Phys.* **1984**, *86*, 257−267.
(50) Xiong, J.-B.; Yuan, Y.-X.; Wang, L.; Sun, J.-P.; Qiao, W.-G.; Zhang, H.-C.; Duan, M.; Han, H.; Zhang, S.; Zheng, Y. S. Evidence for Aggregation-Induced Emission from Free Rotation Restriction of Double Bond at Excited State. *Org. Lett.* **2018**, *20*, 373−376.
(51) Wei, P.; Zhang, J.-X.; Zhao, Z.; Chen, Y.; He, X.; Chen, M.; Gong, J.; Sung, H. H.-Y.; Williams, I. D.; Lam, J. W. Y.; Tang, B. Z. Multiple yet Controllable Photoswitching in a Single AIEgen System. *J. Am. Chem. Soc.* **2018**, *140*, 1966−1975.
(52) Zhao, Z.; Chen, C.; Wu, W.; Wang, F.; Du, L.; Zhang, X.; Xiong, Y.; He, X.; Cai, Y.; Kwok, R. T. K.; Lam, J. W. Y.; Gao, X.; Sun, P.; Phillips, D. L.; Ding, D.; Tang, B. Z. Highly efficient photothermal nanoagent achieved by harvesting energy via excited-state intramolecular motion within nanoparticles. *Nat. Commun.* **2019**, *10*, 768.

https://doi.org/10.1021/cbmi.3c00048
Chem. Biomed. Imaging 2024, 2, 117−125